Advances in Natural Science **ISSN 1715-7862 [PRINT]**
Vol. **3**, No. **2**, **2010**, pp. 139-151 **ISSN 1715-7870 [ONLINE]**
www.cscanada.net **www.cscanada.org**

The 3rd International Conference of Bionic Engineering

A Biomimetic Smart Control of Viscous Drag Reduction

ZHENG X. F.[1]
YAN Y.Y.[2]

Abstract: Viscous flow drag represents the largest contingent of the entire drag that aerodynamic and hydrodynamic devices are subject to. Inspired by the functions of sharks skins, riblet surfaces have been studied and applied to wall structures to reduce turbulent flow drag. However, whilst structural similarity has been obtained it lacks true mimicry. This paper presents an approach of drag reduction using "Smart Surface", a new propose composite surface that combines the riblet with an elastic coating. The "smart surface", inspired by the self-adjustable skin of marine animals such as the dolphin, is designed to modify the traditional riblet technique and enable it to "sense" and interact with the flow by adjusting the wall structure according to the flow condition. Considering the factors of manufacture feasibility, durability and drag reduction performance in previous studies, the physical model of "Smart Surface" is designed. The preliminary establishment of corresponding prediction model has been discussed and calculated. Further work in the aspects of experimental and numerical study of this research is prospected.
Key words: Drag reduction; Elastic coating; Riblet; Self-adjustable; Smart Surface

1. INTRODUCTION

Since energy consumptions increase year after year, energy scarcity has become a critical problem that we have to face in the 21st Century. New and innovative technology is needed to meet energy conservation requirements. High efficiency of energy utilization contributes not only to energy saving, but also to improving the environment. A great deal of attention has been paid to the design and redesign of aerodynamic and hydrodynamic devices such as aircrafts, submarines, long-distance cargo ships, turbine and water pumps for the purposes of promoting the performance by reducing the flow drag during the operations. In the total flow drag that the bodies are subjected to, the component of skin friction drag or viscous drag takes up the largest proportion (Bushnell, 1983).

[1] Energy and Sustainability Research Division, Faculty of Engineering, University of Nottingham, Lenton Firs Building, University Park, Nottingham NG7 2RDUK, UK.
[2] Corresponding author, Energy and Sustainability Research Division, Faculty of Engineering, University of Nottingham,Lenton Firs Building, University Park, Nottingham NG7 2RDUK, UK.
Email: yuying.yan@nottingham.ac.uk.
*Received 10 May 2010; accepted 18 July 2010

Viscous drag has been considered one of the major barriers to further optimization of most aerodynamic and hydrodynamic devices. In the long term, significant drag reduction can contribute immensely to the achievement of energy saving. Even a small amount of drag increase can have a great economic impact if a large number of units are involved.

A major proportion of the drag of streamlined vehicles and vehicles with large surface areas is due to the surface shear, so any reduction in the skin friction will produce more efficient vehicles by lowering fuel consumption and/or raising cruising speeds. Taking airlines as an example, shortages and rising costs of energy have necessitated new researches directed toward the viscous drag reduction of turbulent boundary layers. Drag reduction for aerial vehicles has a number of positive effects, namely, reduced fuel consumption with associated economic and environmental consequences, larger flight range & endurance and higher achievable cruise speeds. Even viscous drag reduction of 5-10% on the fuselage alone is significant when these small reductions can be translated into a fuel saving in the order of magnitude of half a billion dollars annually (Bushnell & Hefner, 1989).

Turbulent flow has been the kernel flow regime that the drag reduction researches have focused upon. In the pursuit of a drag reduction technique with high efficiency and great performance, insights have been taken from the nature in an effort to look for answers to controlling drag reduction in a more effective way. Since the nature has a clear priority for the development of drag-reducing surfaces, the evolved abilities and characteristics of creatures are the sources of inspiration which enable researchers and engineers to find a better way of creating remarkable designs and solving technical problems.

For the low-drag-oriented characteristics in the nature, studies (Gray, 1936; Kazuhiro & Junichiro, 2000; Walsh & Weinstein, 1978; Adkins &YAN, 2006; Balasubramanian et al., 1977; Bannasch, 1997) have been carried out to investigate the special structures shown in the skin of marine animals such as the shark, dolphin, seal and penguin as their "talents" are believed to be due to their skin architectures. Riblet surface, inspired by the skins of fast sharks, has been seen as an effective turbulent drag reduction method which reduces flow drag by changing the position of the origin of velocity profile. However, the riblet surfaces adopted so far only give a limited range of drag reduction due to the rigid structures which bear the flow passively. A "smart surface", consisting of trapezoidal riblet and elastic coating, is designed to widen the range by enabling the wall surface to be self-adjustable, to interact with the boundary layer under different flow conditions and adjust the wall structure accordingly.

In this paper, an overview of the common methods of turbulent flow drag reduction and shark-inspired surface-riblet for drag reduction is presented first. Then, the "smart surface" is suggested and discussed in an attempt to approach the advanced biomimicry.

2. DRAG REDUCTION IN INTERNAL FLOW

Internal flow is a flow for which the fluid is confined by a surface. Due to the presence of a fully developed velocity profile which is independent of position, blocking has a dominant effect. The most common techniques that have been adopted in the drag reduction researches for internal flow include the employments of riblet, particle, and surfactant, as well as polymer solutions.

Riblet surfaces have been well known as an outstanding passive drag reduction technique in turbulent flow. They are surfaces with micro-grooves aligned with the mainstream direction. According to the shape of the cross section, riblets can be classified into three basic categories: v-groove riblet, rectangle riblet and semi-circular riblet. Other riblets with different cross-section shapes such as spaced v-grooved riblet, valley/peak curved v-grooved riblet, scalloped riblet and finite blade riblet derive from the three basic categories. In early years, many experimental and numerical investigations (CHU & Karniadakis, 1993; CHU & Karniadakis, 1991; Choi) have been focused on dealing with internal duct/pipe-type flows. Its drag reduction capability in internal flows has been controversial (Choi; John et al., 1983; Orlandi & Factica, 1997).

Based on the use of a stabilizing body force, the technique of particle addition is able to reduce turbulent drag which has been proved by the following three types of experiments: gas-solid suspensions,

liquid-nonfibrous suspensions and liquid-fibre suspensions. Due to the complicating effects of changing gross fluid density, simultaneous transport of two or more materials, flow orientation, the phenomenon definition of drag reduction by particle addition has been discussed mainly in the case of internal flow.

Polymer solutions are liquid mixtures made of long macromolecular chains, and small, light molecules of solvent. Since much attention has been attracted by drag reduction observed in turbulent flow of polymer solutions (Motoyuki et al., 2006; Tulin, 1984), a number of theories have appeared to explain how polymer molecules interfere with production, growth or transport of turbulent disturbances.

Surfactants are wetting agents that lower the surface tension of a liquid. It allows easier spreading and lowering of the interfacial tension between two liquids. Surfactant solutions hold the drag reduction capability in a limited range of Reynolds number. The main feature of surfactant solutions' friction behaviour is the disappearance of drag reduction effect when a critical wall stress is reached (Shenoy et al., 1984).

3. DRAG REDUCTION IN EXTERNAL FLOW

External flow is a flow whose boundary layer is not constrained by adjacent surfaces. The state of the flow is not fully developed and blocking does not exist. Friction takes place in an ever-growing boundary layer and consequently the drag is determined by the thickness of final boundary layer. Since many aerodynamic and hydrodynamic applications involve with external flow, the drag reduction research has become increasingly necessary and active.

3.1 Active control

For active control, turbulent drag reduction can be achieved by changing the flow properties or behaviour. The former can be realised by adding extra substances into the flow, which includes bubble, particle, polymer solutions and surfactant (referred as "additives"). The latter can be done by imposing external force and mass, such as Magnetohydrodynamic (MHD) control and mass injection.

Air lubrication is one of active methods. Injecting microbubbles into the boundary layer on a solid wall can reduce skin friction significantly due to the lower density and viscosity of the gas layer formed by microbubbles. Based on alteration of the wall boundary condition, this approach, called "air lubrication", is suitable for liquids only and involves placing a gas "slip layer" between the wall surface and the liquid. Since its first report (Gaster, 1988), it has been used to decrease the drag that large ships go through (Foeth; Jimenez & Pinelli, 1997; Yoshiaka et al., 2000) in the purpose of reducing operating costs as well as greenhouse gas emissions.

The wall surface mass transfer is classified to two categories, one is slot mass injection; the other is called distributed normal injection. The directions of these two mass injection approaches are tangential and normal to the wall surface. Due to the injecting direction and the normal injection are somewhat similar to those of adverse pressure gradient. The mean longitudinal velocity profile in the vicinity of the wall can become highly inflected and result in an increase of the turbulence intensity (Woolridge & MuzzY, 1966).

The principle of electromagnetic control is based on the electromagnetic force (Lorenz force) produced by an electromagnetic field. The force acts on a flowing fluid electrically to produce drag reduction effect. The complicated interactions between the force and turbulent flow have been studied (Chapter, 1998) and applied onto the body of submarine to prevent the turbulence production.

In addition, bio-fouling control aims at maintaining low drag by preventing the formation of fouling layer, consisting of slimes and small barnacles which were found to cause a four-fold increase in resistance on a tested towing tank compared to the original clean status (Swain, 1998).

3.2 Passive control

Involved with the wall modification by changing the wall structure and adjusting attack angle, passive control includes the employments of riblets, large eddy breakup device (LEBD), convex curvature, wavy wall and adverse pressure gradient. Compared to active control, the advantage of passive control is reducing the viscous flow drag in a passive way where the drag reduction effect is immensely shown under certain designed flow conditions.

Among all the methods in passive control, the technique using riblets surface is the method that has been studied most widely and extensively. The actions of riblet surface on internal flow and external flow can be different due to the different level to which the velocity profiles are developed. Because of the demands of aerodynamic and hydrodynamic applications such as airplanes, submarines and racing yachts, riblets' application of greatest interest lies in external flows in recent years. More details are presented in the next chapter.

Large eddy breakup devices (LEBU) constitute probably the most promising single recent development in turbulent drag reduction. Studies (Schlichting, 1979; Garc´ıa & Jim´enez, 2008; LAI &YAN,2001) show that the thickness of shear layer and the magnitude of the Reynolds shear stress were reduced by the application of LEBU. Skin friction reduction was obtained in the downstream of LEBU.

Convex curvature and wavy walls are also the methods of passive control. The effects of convex curvature are very favourable to large decreases in turbulence intensity and skin friction. This structure is found on the penguin skin (Balasubramanian et al., 1977; Bannasch, 1997). There exist indications that the convex curvature affects primarily the large, outer eddies just like LEBU. The original impetus for the wavy wall studies at Langley (Cary et al., 1979; Anders et al., 1984) was the apparent average skin friction reductions obtained by Kendall and Sigal over wavy walls.

The other passive control is concerned with adverse pressure gradient which occurs when the static pressure increases in the flow direction. Mathematically this is expressed as: $dP/dx > 0$. When flow reversal occurs, the flow is said to be separated from the surface. This drag reduction approach aims at reducing the near wall longitudinal momentum in an extremely straightforward way by retarding the flow near the wall.

3.3 Interactive control

Interactive control is defined as observing the coherent turbulent structure and controlling turbulent boundary layer by adopting physical or thermal activities in wall surfaces, includes wall oscillation, wall heating/cooling and compliant wall.

Since wall oscillation was found to be capable of reducing skin-friction drag in turbulent boundary layer by altering the boundary layer structure, many studies (Choi, 1997; Choi, 1998; John et al., 1986; Chung, 1985; Berman, 1985; Orlandi, 1997) have been carried out to seek the drag reduction mechanism of wall oscillation experimentally and theoretically. Laadhari (Chung, 1985) observed viscous drag reduction by detailed tests using hot-wire anemometry which was proved by Choi (Choi, 1997; Choi, 1998). Same effect was observed by Orlandi (Berman, 1985; Orlandi, 1997) in numerical studies.

Wall heating/cooling, which has been found to be able to reduce drag on the basis of a stabilizing body force (Bushnell, 1982), could conceivably be of interest on aircraft utilizing liquid hydrogen fuel where a sizable heat sink is readily available. In a large scale low speed boundary layer experiment, wall cooling provided 18% of the skin friction reduction (Bushnell,1983).

In addition, the concept of compliant wall is inspired by cetaceans which seem to possess the ability of reducing body drag when they swim at high speeds. Many studies (Cooper & Carpenter; Cooper & Carpenter; Choi et al., 1994; Gary, 1980; Kramer, 1937; Steuben & Krefft, 1978; Djenidi et al., 1989; Laadhari, 1994) have been carried out to find the answer to explain this talent shown by dolphins. Kramer's up to 60% drag reduction experiment which shows dolphin skin as compliant wall has been proved and also opposed by the studies carried out at different time. But most researches have agreed with the fact that compliant walls are able to reduce drag in turbulent flow. Due to the tremendous density difference between gaseous flow and the wall materials, this approach is mostly confined to water for net drag reduction.

The interactive and active controls achieve drag reduction in a controllable way suitable for varying flow conditions, while passive control is suited for designed flow conditions due to the passive style of bearing flows. Considering the input of extra power or mass, passive control is more energy-saving than interactive and active controls due to the absence of extra input.

4. SMART CONTROL OF DRAG REDUCTION

The smart control method is proposed for reducing drag of external flow. Reif (Reif, 1978) found that the fast-swimming sharks (the oldest fish in terms of their evolutionary history) had scales with finely spaced ridges, basically aligned with the local flow. Due to this special structure, a fast-swimming shark is capable of maintaining the flow drag around its body at a low level even at high swimming speeds. As a shark-inspired drag reduction approach, riblet has been found to be capable of reducing turbulent drag. Typical applications in engineering are seen such as airplane fuselage, competition boat and swimming suit for wall modification.

Among the turbulent drag reduction techniques, riblets have been the most widely investigated method of drag reduction (Walsh, 1983). Over the last 60-70 years, it has been widely and intensively investigated from a wide range of aspects. Riblets with the shapes of rectangular, triangular, semicircular, trapezoidal, and scalloped-shape have been studied in terms of the drag reduction performance. In addition, the impact of the geometry variation of riblet surface on the drag reduction has also been investigated (Merkle & Deustch, 1992). Obviously most of studies carried out so far have been directed towards the turbulent flow drag reduction. Conclusions widely agreed by many of the relevant studies have been drawn that the drag reduction effect in turbulent flow is related to the dimensionless geometries of riblet structure.

Fig. 1(a) shows the riblet drag reduction that is plotted by previous studies (CHU & Karniadakis, 1991; Walsh, 1983; Bechert et al., 1997; Bechert & Bartenwerfer, 1989; Bechert et al., 2000). Most of them focused on the studies of drag reduction performance in turbulent flow, but there was a blank in laminar flow until the later studies (Choi; Orlandi & Factica, 1997; Laadhari, 1994; Douglas et al., 2004) which looked into the riblet drag reduction in laminar flow and agreed with the drag increase in laminar flow (see Fig. 1(b)). The range of dimensionless spacing s^+ for drag reduction is limited to certain area which varies with the riblet architecture. Other geometries such as riblet valley, peak and groove shape can also affect the performance apparently (Merkle & Deustch, 1992). It is difficult to widen the range of drag reduction since the riblet is made of materials with high rigidity. Therefore, in order to gain a wider range, the geometries should be flexible to be better-fitted and well performing in a wider range of flow regime. In the following part of this article, “Smart Surface”, which is expected to take the flexible riblet on board, is introduced.

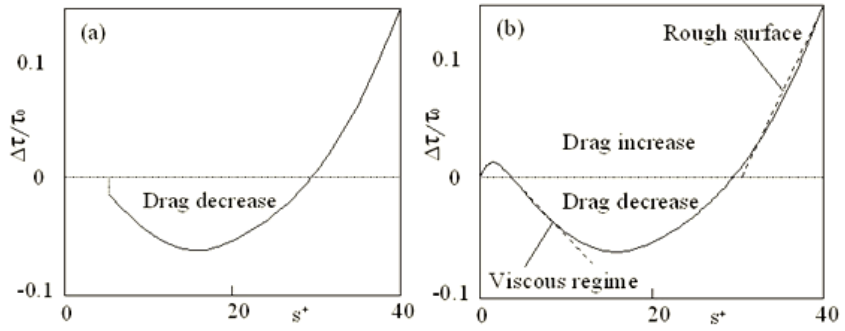

Fig. 1: Relation curve of drag reduction $\Delta\tau/\tau_0$ and non-dimensional riblet spacing s^+. (a) Previous drag reduction curve, (b) Modified relation curve

In Fig. 1 caption, Reynolds number for the riblets s^+ is defined as usual, $s^+ = su_\tau / v$, s is the lateral rib spacing, $u_\tau = (\tau_0 / \rho)^{1/2}$, τ_0 is the difference of the shear stresses between test plate and smooth reference plate, $\Delta\tau = \tau - \tau_0$, negative value of $\Delta\tau$ means drag reduction.

4.1 Smart surface

As a well known drag reduction method, riblet is originally inspired by fast-swimming sharks which can be dated back to 350 million years ago. Apart from sharks, other marine animals like penguin, seal and dolphin, have also attracted researchers' attention and interest. Riblet-like structure has been found on the seal fur by Motoyuki[14], the surface shows better drag reduction performance than the trapezoidal riblet used in the study[14]. For dolphin's capability of keeping lower drag at high swimming speed, researchers (Gray, 1936; Orlandi & Factica, 1997; Carpenter & Garrard, 1985; Shinsuke et al., 2006) have focused on the physical architecture of dolphin skin by studying its performance on the imitated "dolphin skin" in both experimental and theoretical ways. They showed the expected trends but didn't reach the biological level. However, the previous studies lead us to a fact that just physical imitation is not enough to immensely express the characteristics and abilities shown by the natural "objects" or "processes". Except for the strengths of physical structures found on different creatures, most of them have one common ground that they are self-adjustable rather than passive bearer of external conditions.

Presented here with self-adjustable design, the "smart surface" consists of riblet and elastic coating which act as the basis and elastic layer, respectively. Unlike the wall surface mounted with traditional riblets which purely bear the flow over them passively, this "smart surface" enables the wall surface to interact with the boundary layer and adjust the wall structure accordingly.

4.2 The physical model

Despite the blade riblet surface could have the biggest space for self adjusting, its durability and manufacture difficulty make it impractical to be adopted in "smart surface". Trapezoidal riblet surface, which shows the closest similarity to blade riblet surface and has good durability and manufacture implement, is used as the basis of "smart surface". It also allows crack inspection through the flat valley surface when the elastic coating is transparent. The final physical model is designed and shown in Fig. 2.

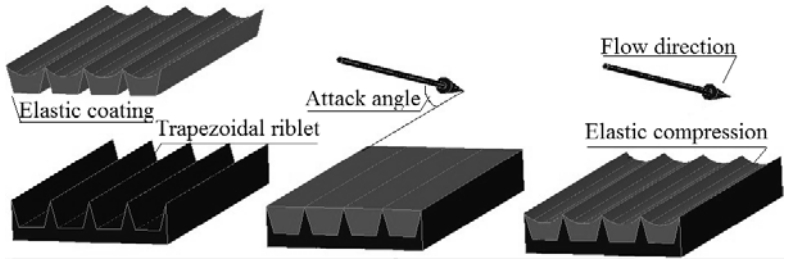

Fig. 2: Structure of "smart surface", (a) the components (b) Before compressed, (c) After compressed

The concept of its working mechanism is shown in Fig. 3. Prior to the occurrence of the compression, the surface keeps the smooth contour which is beneficial for maintaining the laminar flow drag at a low level. When the flow develops into turbulent, the drag on smooth surface will be increased to a higher level compared to laminar flow. In this case, the "smart surface" adjusts its surface according the flow velocity to keep itself in a condition which enables a more effective drag reduction in a wider flow range. The self-adjusting is not an abrupt case but a gradual change. The key issue is to make sure the extent of self-adjustment meets the requirement of effective drag reduction. Either premature or overdue adjustment would increase the flow drag oppositely if it is not designed reasonably.

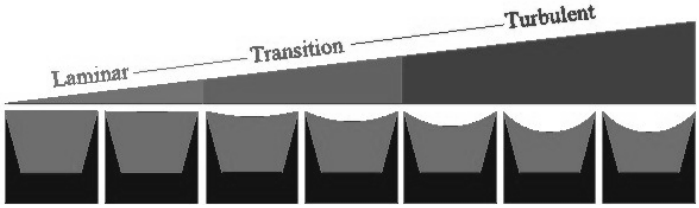

Fig. 3: Compressions under different flow regimes

In this drag reduction regime, the elastic coating is supposed to sense the flow velocity and carry out the according action. Namely, a zero attack angle needs to be avoided. Hence, the attack angle of flow and the material of elastic layer determine the sensibility of "Smart Surface" to flow variations. The way that these two factors impact on the drag reduction performance needs to be understood.

The material with smaller bulk modulus and the flow with higher attack angle both give the surface a higher sensibility. For a given flow condition, the right sensibility needs to be obtained to achieve an optimum drag reduction performance. When the sensibility is too high, a significant compression would take place before the flow transfers into turbulent. When the attack angle is too high, the separation is more likely to happen. Unreasonable sensibility designs would create unfavourable conditions for the overall drag reduction.

4.3 The prediction model

Mathematically, this motion can be described as the motion of an elastic solid which moves and interacts with an incompressible viscous fluid under the conditions of continuity of the velocity fields and normal components of the stress tensors along the moving interface between the two phases. Before described specifically by the accurate mathematical model, the performance of "smart surface" in viscous regime is firstly predicted by the prediction model in an attempt. Basically, solving mathematical model of "smart surface" involves two major issues which include drag reduction and elastic compression, respectively.

Proposed by Luchini (Luchini et al., 1991) and modified by Bechert (Bechert et al., 1997), equation (1) shows essential trend with the experimental test in terms of initial slope of drag reduction.

$$\frac{\Delta\tau}{\tau_0} = -\frac{0.785(\Delta h/s)s^+}{(2c_f)^{-1/2}+1.25} \tag{1}$$

where $c_f = 0.0791(\frac{\bar{u}d}{v})^{1/4}$ (Schlichting, 1979).

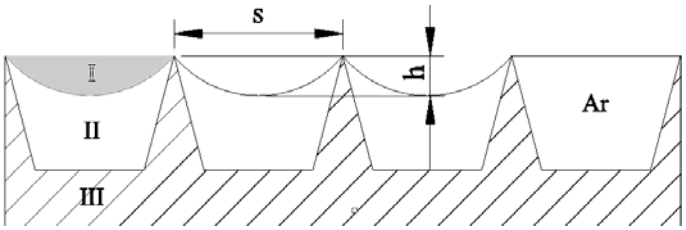

Fig. 4: Equivalent model of compressed surface
(I: riblet cross section; II: Elastic coating;
III: Trapezoidal riblet)

Suppose the riblet cross section is a segment of a circle. The chord length and arch rise are *s* and *h* respectively (see Fig. 4). Then, the riblet cross section area A can be expressed by

$$A = \frac{\pi\left(\frac{s^2+4h^2}{8h}\right)^2 \arcsin\frac{4sh}{s^2+4h^2}}{180} - \frac{s^3-4sh^2}{16h} \tag{2}$$

(Equation (2) is valid only when the segment I is smaller than the half circle)

Elastic compression

For a given flow condition, the Reynolds number is directly determined by flow velocity. To ensure the "smart surface" is compressed according to the flow condition, the zero attack angles must be avoided. Axis X, Y and Z denote the streamwise, wall-normal and spanwise direction, respectively. Supposing the riblets are aligned accurately in the streamwise direction, the stress model can be divided into two planes, YZ plane and XY plane, see Fig. 5.

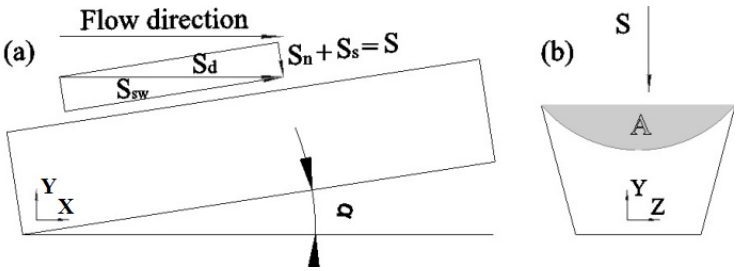

Fig. 5: Stress analysis (a) XY plane, (b) YZ plane

Provided the flow attacks the surface at the velocity v with an angle of α, the stress S_d on the surface caused by the flow can be decomposed into normal stress S_n and shear stress S_{sw}, $d\sigma$ is the finite area. S_{sw} is ignored due to its non-contribution to self-adjusting. Therefore, the overall normal stress that $d\sigma$ bears can be expressed by

$$dS = dS_n + dS_s = (P_s + \frac{1}{2}\rho v^2 \sin\alpha)d\sigma \tag{3}$$

where P_s is the static pressure, $P_d = \frac{1}{2}\rho v^2$.

The compression is a process of volume decrease which is caused by the pressure imposed by the flow over the surface. For a given material of elastic coating, the volume decrease can be calculated by bulk modulus K under certain pressure. It can be formally defined by the equation:

$$K = \frac{PV}{\Delta V} \tag{4}$$

where P is the pressure normally imposed on the surface. V and ΔV are the volume of filled elastic material in riblet grooves and volume decrease caused by compressions, respectively.

For the compression of elastic coating in this modelling, due to the confinement of riblet structure, the compression in the streamwise direction is ignored. ΔV can be replaced by riblet cross section area A, the equation of bulk modulus K can be simplified to

$$K = \frac{P}{A/A_r} \tag{5}$$

where A_r is the cross section area of the trapezoidal riblet. A is designed to be zero when the flow state is still. For a given material of elastic coating, K is known. Therefore, $A = \frac{A_r P}{K}$, where $P = P_s + P_d$ is

the normal pressure imposed on the surface of elastic coating, P_s is the static pressure. Provided the elastic coating stays in smooth condition when $P = P_s$, then the compression is caused by dynamic pressure, $P = \frac{1}{2}\rho v^2 \sin\alpha$.

A can be calculated by

$$A = \frac{0.5 A_r \rho v^2 \sin\alpha}{K} \tag{6}$$

where ρ, v, and α are the fluid density, flow velocity, and flow attack angle.

From equations (2) and (6), the spacing height h under different flow velocity can be calculated. Combined with the relationship of protrusion height $\Delta h / s$ and riblet height h / s (Bechert et al., 1997), the drag reductions caused by different flow velocities can be obtained from equation (1).

4.4 Predictions

At the present research stage, the specific parameters in the model haven't been finalised. However, in order to predict the general trend of drag reduction achieved by "Smart Surface", the required parameters will be given designed values on the basis of real case. Fig. 6 shows the cross section of a closed water channel ($150mm \times 150mm$) in which a shuttle ($d = 50mm$) is set at the center of cross section. It is coated with "Smart Surface".

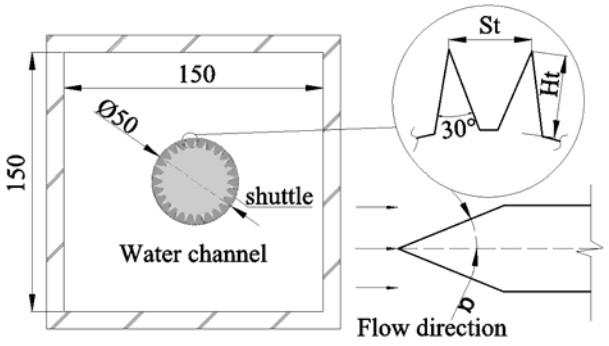

Fig. 6: Test shuttle with "Smart Surface" in water channel (S_t and H_t are the spacing and height of trapezoidal riblet)

The assumptions are as follow: 1) Drag reduction of $\alpha = 6^\circ, 12^\circ, 18^\circ, 24^\circ, 30^\circ$, are calculated with $K = 5\times10^3$ Pa, respectively. Meanwhile, the same procedure is carried out with bulk modulus $K = 5\times10^3$, 6×10^3, 7×10^3, 8×10^3, 9×10^3, 10×10^3 Pa when $\alpha = 30^\circ$. 2) The friction velocity u_τ is 10% of the average velocity $\bar{u}$. 3). The elastic material is compressed in the range of linearly elastic regime. 4). The flow around the shuttle doesn't separate.

The relationship between riblet height h and non-dimensional riblet spacing s^+ can be obtained from Equation (1). As shown in Fig. 7, h is increased by the growing flow velocity which imposes larger pressure on "Smart Surface". The increased value is determined by K.

Fig. 8 shows the trend of the initial slope of drag reduction given by "smart surface" with different K. Bigger K value gives larger drag reduction and drag reduction slope.

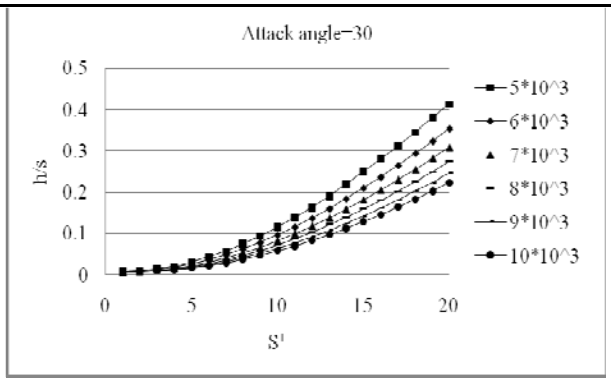

Fig. 7: The relation curve of h/s and s^+ with different bulk modulus

Compared to the traditional predicted curve which gives invariable slope of drag reduction, Fig.8 indicates increasing drag reductions could be obtained when the flow velocity increases.

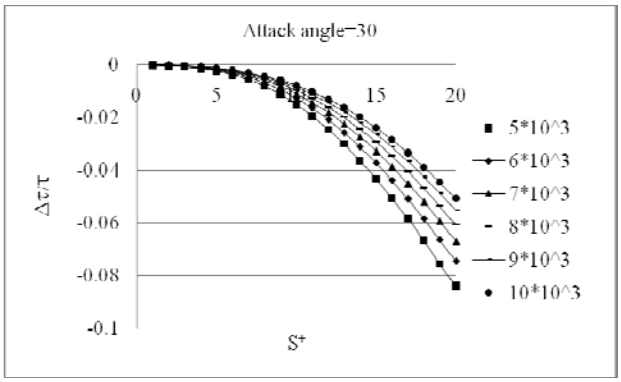

Fig. 8: Initial slope of drag reduction obtained from "Smart Surface" under different bulk modulus K

From Fig. 9, the role that the attack angle plays in drag reduction can be understood generally. The bigger attack angle gives a larger drag reduction. However, form drag would be increased when the attack angle is too large. Attention needs to be paid to the impact of flow separation which is likely to happen when the flow attacks the surface with a certain angle due to the adverse pressure gradient.

Due to the hypothetical conditions, it doesn't necessarily mean that it represents the actual trend of real case. Further experimental and numerical research work needs to be approached to verify the validity.

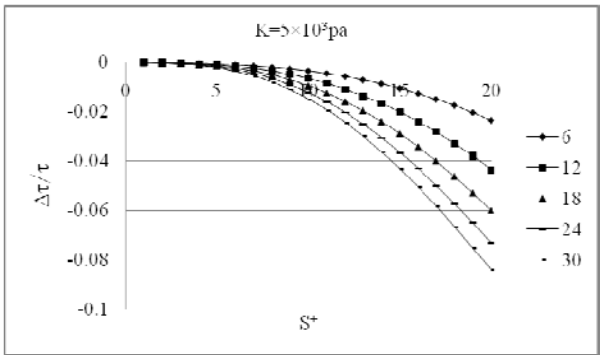

Fig. 9: Initial slope of drag reduction under different flow attack angles α

5. CONCLUSIONS AND PROSPECTS

Drag reduction techniques have been reviewed from the aspects of internal flow and external flow. Due to the roles that the fluid and wall play in the drag reduction mechanism, the approaches for external flow have been classified into active, passive and interactive controls, respectively. Inspired by the low-drag-oriented characteristics in nature world, the previous biomimetic method for reducing drag is introduced and analyzed. Based on this, the "Smart Surface" is proposed and aimed at advanced mimicry of self-adjustable surface for drag reduction in external flow. The preliminary concept of physical and prediction models presented here are for further modification of the prediction model and the development of mathematical model. Meanwhile, insights must be shed onto the detailed study of significant factors such as the compression mechanism of elastic coating, flow separation and self-adjusting design. Experimental and theoretical means will be employed to verify the applicability in future work.

REFERENCES

A. J. Cooper & P. W. Carpenter. J. *Fluid Mech. 350*, 231–259.

A. J. Cooper & P. W. Carpenter. J. *Fluid Mech*. 350, 261–270.

A.M. Cary, L.M. Weinstein, D.M. Bushnell. (1979). Viscous flow drag reduction, vol. 72. Presented at the symposium on viscous drag reduction, Dallas, Texas, pp.144-167.

AV Shenoy. (1984). Colloid & Polym. *Sci., 262*, 319.

C.E. Woolridge and R.J. MuzzY. (1966). *AIAA Journal, vol. 4, No.11*, Nov. PP. 2009-2016.

Chapter. (1998). "Proceedings of the International Symposium on Seawater Drag Reduction." *Newport, Rhode Island*, pp. 359 *(July)*.

CHU D. and G. E. M. Karniadakis. (1993). A direct numerical simulation of laminar and turbulent flow over riblet-mounted surfaces. *J. Fluid Mech., 250*: 1-42.

CHU D. and G.E. Karniadakis. (1991). Numerical investigation of drag reduction in flow over surfaces with stream aligned riblets. *29th Aerospace Sciences Meeting, AIAA Paper 91-0518*.

Choi, K-S.et al.. (1997b). Turbulent boundary layer control by means of spanwise-wall oscillation. A*IAA Paper 97-1795*.

Choi, K-S.et al.. (1998). Turbulent boundary-layer control by means of spanwise-wall oscillation. *AIAA J. 36 (7)*, 1157-1163.

Choi, H., Moin, P.& Kim. (1994). Active turbulence control for drag reduction in wall-bounded flows, *J. Fluid Mech. 262*, 75-110.

CHUNG KH, PhD. (1985). Thesis "Composite compliant coatings for drag reduction utilizing low modulus high damping silicone rubber".

Douglas Chu, Ron Henderson and George Em Karniadakis. (2004). Parallel spectral-element—Fourier simulation of turbulent flow over riblet-mounted surfaces. *Physics and Astronomy, vol.3*: 219-229.

D.W. Bechert, M. Bruse, W. Hage, J.G.T. (1997). Van der Hoeven, and G. Hoppe. J. Fluid Mech.. 338:59-87.

D.W. Bechert and M. Bartenwerfer. (1989). The viscous flow on surfaces with longitudinal ribs. *J. Fluid Mech., 206*: 105-129.

D.W. Bechert, M. Bruse, W. Hage. (2000). Experiments with three-dimensional riblets as an idealized model of shark skin. *Experiments in Fluids 28:* 403-412.

D. Adkins, YAN Y.Y. (2006). *CFD simulation of fish-like body moving in viscous liquid, 3(3)*, 147-153.

D.M. Bushnell. (1983). Turbulent drag reduction for external flows. *AIAA 21st Aerospace sciences Meetings.* 10-13, January.

D.M. Bushnell, J.N. Hefner. (1989). Viscous drag reduction in boundary layers. *American Institute of Aeronautics and Astronautics, Vol. 123*.

E.J.Foeth, *Decreasing frictional resistance by air lubrication*, 20th international Hiswa Symposium on Yacht Design and Yacht construction.

Gray J. (1936). Studies in animal locomotion. VI. The propulsive powers of the dolphin. *J Exp Biol 13*, 192-199.

Gary R. Hough. (1980). *AIAA progress in astronautics and Aeronautics*, vol.72.

G Swain. (1998). in "Proceedings of the Int. Sym.on Seawater Drag Reduction." *Newport, Rhode Island*, pp. 155 *(July)*.

H. Choi. On the effects of riblets in fully developed laminar channel flows. *Physics of Fluids A3 (8).*

H. Schlichting. (1979). *Boundary Layer Theory* (trans. J. Kestin), 7th edn. McGraw-Hill.

J.B. Anders, J.N. Hefner and D.M. Bushnell. (1984). Performance of large-eddy breakup devices at post-transitional Reynolds numbers. *AIAA, Aerospace Sciences Meeting*, 22nd, Rno, NV, Jan. 9-12. 10p.

J. Jimenez and Pinelli, A.. (1997a). Controlling the structures of the turbulent wall region. Proceedings Euromech Colloquium-361, Berlin.

John J.J. Chen, Yiu-Cheong Leung and Normal W.M.Ko. (1986). Drag reduction in longitudinally grooved flow channel. Ind. Eng. *Chem. Fundam., 25*, 741-745.

John C. Lin, L.M. Weinstein, R.D. Watson and R. Balasubramanian. (1983). *Turbulent drag characteristic of small amplitude rigid surface waves*. Presented at the AIAA 21st Aerospace Sciences Meeting, Reno, Nevada, January 10-13. Paper No. 83-0288.

Kazuhiro Fukuda, Junichiro Tokunaga. (2000). Frictional drag reduction with air lubricant over a super-water-repellent surface. *J Mar Sci Technol 5*: 123-130.

Kramer, M. (1937). *Einrichtung zur Verminderurg des Reibungswide stands* (Device for Reducing the Frictional Resistance), German Patent No. 669897, March 17.

K.S. Steuben, G. Krefft. (1978). Die haie der sieben Meere. Hamburg: Verlag paul Parey. (The sharks of the seven oceans.)

Laadhari, F et al.. (1994). Turbulence reduction in a boundary layer by a local spanwise oscillating surface. *Phys. Fluids A6(10)*, 3218-3220.

LAI H, YAN Y.Y.. (2001). The effect of choosing dependent variables and cell-face velocities on convergence of the SIMPLE algorithm using non-orthogonal grids. *International Journal of Numerical Methods for Heat & Fluid Flow, 11(5/6)*, 524-546. Emerald.

L. Djenidi, J, Liandrat, F. Anselmet, L. Fulachier. (1989). in *Advances in Turbulence 2*, edited by H.–H. Fernholz and H. E. Fiedler (Springer-verlag, Berlin,), pp. 438-442.

Merkle, C.L., Deustch, S.. (1992). *Applied Mechanics Reviews 45 (3)*, 103-127.

M. J. Walsh. (1983). Riblets as a viscous drag reduction technique. *AIAA Journal, vol.21, No. 4, April.*

M. J. Walsh and L.M. Weinstein. (1978). *AIAA Paper* 78-1161, *July*.

M Gaster. (1988). in "Turbulence Management and Relanimarisation" (HW Liepmann and R Narasimha eds), Spinger-Verlag, Berlin, p. 285.

Motoyuki Itoh, Ryo Iguchi, Kazuhiko Yokota, Norio Akino, Ryutaro Hino, Shinji Kubo. (2006). Turbulent drag reduction by the seal fur surface. *Physics of Fluids 18*, 065102.

MP Tulin. (1984). in "Proceedings of the 3rd International Conference on Drag Reduction" (RHJ Sellin and RT Moses, eds), Bristol, UK, University of Bristol, Bristol, UK.

NS Berman. (1985). *The influence of polymer additives on velocity and temperature fields* (B Gambert ed.), p 293, Springer-Verlag, Berlin.

Orlandi, P., Factica, M.. (1997) *J. Fluid Mech.. 343*, 43-72.

Orlandi, P.. (1997). Helicity fluctuations and turbulent energy production in rotating and non-rotating pipes. *Phys. Fluids 9 (7)*, 2045-2056.

P. Luchini, F. Manzo, & A. Pozzi. (1991). Resistance of a grooved surface to parallel flow and cross-flow. *J. Fluid Mech. 228*, 87-109.

PW Carpenter and AD Garrard. (1985). *J. Fluid Mech. 155*, 465.

R. Balasubramanian, Aubrey M. Cary, Dennis M. Bushnell and Robert L. Ash. (1977). *Fifth biennial symposium on turbulence*. University of Missouri-Rolla, October.

R. Bannasch. (1997). Experimental investigations on the boundary layer development in swimming penguins: mechanisms of drag reduction and turbulence control. *Proceedings of the 10th European Drag Reduction Meeting*. Berlin.

R. Garc´ıa Mayoral and J. Jim´enez. (2008). Tech. Rep. MF-083, *Sch.l of Aeronautics*, Madrid.

Shinsuke Mochizuki, Seiji Yamada and Hideo Osaka. (2006). *JSME International Journal Series B, vol. 49, No.4 Special Issue on Jets, Wakes and Separated Flows*, pp. 921-927.

W.E. Reif (1978). *Protective and hydrodynamic function of the dermal skeleton of elamolranshs. Vol. 157,* pp. 184-187.

Yoshiaka Kodama, Akira Kakugawa Takahito Takahashi, Hideki Kawashima. (2000). *International Journal of Heat and Fluid Flow 21:* 582-588.